The Fifth International Conference on Railway Technology
RAILWAYS 2022
22–25 August 2022
Montpellier, France

Proceedings of the Fifth International Conference on
Railway Technology:
Research, Development and Maintenance
Edited by J. Pombo
Civil-Comp Conferences, Volume 1, Paper 22.1
Civil-Comp Press, Edinburgh, United Kingdom, 2022, doi: 10.4203/ccc.1.22.1

Effects of a varying track and soil stiffness on ground vibrations near railway lines

L. Auersch

Federal Institute of Material Research and Testing, Berlin, Germany

Abstract

Usually, geometric irregularities are considered as the main cause of ground vibrations from trains. A varying stiffness of the track, the track support and the soil can also generate ground vibrations. The regular stiffness variation of the track on and between the sleepers results in a deterministic dynamic axle load. The random stiffness variation of the track support yields also dynamic axle loads which are generated by the acceleration of the unsprung mass (from the varying wheel displacements under the static axle load). The random stiffness variation has a second effect. The pulses from the passage of the static axle loads are superposed regularly to the quasi-static response, but also irregularly to yield a "scattered" part of the axle pulses. The same holds for a random variation of the soil stiffness. All these effects of stiffness variations have been calculated by wavenumber-domain multi-beam track models, a random finite-element soil model and the superposition of axle impulses in a stochastic simulation. The results are confronted with many measurements at different sites. It is concluded that the stiffness variation of the track and the soil generate an important ground vibration component near railway lines.

Keywords: Ground vibration, axle loads, irregularities, varying stiffness.

1 Introduction

In many measurements of railway-induced ground vibration, a certain mid-frequency component (8-30 Hz for normal train speeds, 16-50 Hz for high-speed trains) is dominating the mid- and far-field amplitudes (distances $x > 10$ m). Early observations from the ICE test runs can be found in [1,2] where also first interpretations have been given, and in [3] the mid-frequency component has been named “axle-distance excitation” and indicated as the second important component besides the “sleeper-distance excitation” [4]. Later on, more measurements of BAM in Germany and Switzerland [5] and of other institutes [6] have also revealed this component, see for example [7] und Spain [8] in Figure 1. It has been found that this component is shifted in frequency when the train speed is increased [9,10], but the increase of amplitudes can be from constant to strongly increasing [7]. Sometimes, the reduction of this component by a ballast-plate track [6], a trough with under ballast mat [11], a slab track [12] or a tunnel track could be observed. The purpose of the present work is to find the reason of this component and to compare it with other effects of a varying stiffness or a moving static load. The reasons have been searched in vehicle dynamics [13], the static axle loads passing regularly over the track (the quasi-static response) [14-16], the geometric irregularities of the vehicle (wheel) and the track and the corresponding dynamic loads [17], the regular and irregular dynamic loads from stiffness variations of the track [4,10,12,18], and the irregular wave propagation due to stiffness variations of the track support [13,19] or the soil [1,20]. The trans-Rayleigh train effect [21], however, has been excluded because none of the 50 BAM-measuring sites had a wave velocity that is lower than the train speed. All the effects of stiffness variations have been calculated by wavenumber-domain multi-beam track models, a random finite-element soil model and the superposition of axle impulses in a stochastic simulation.

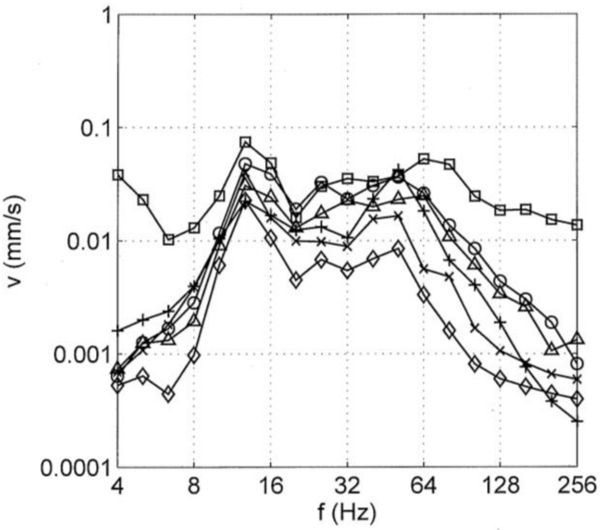

(a)

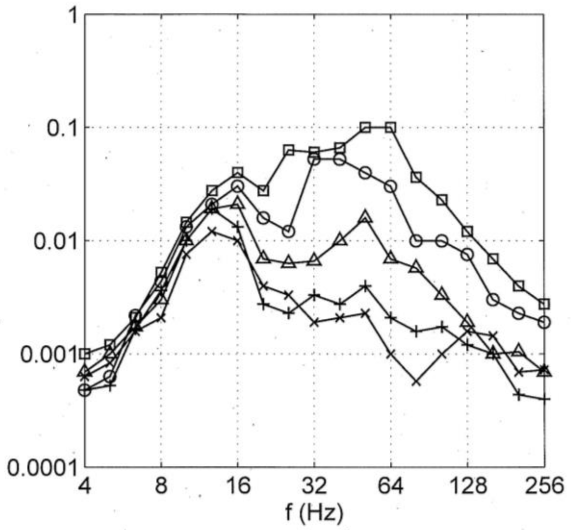

(b)

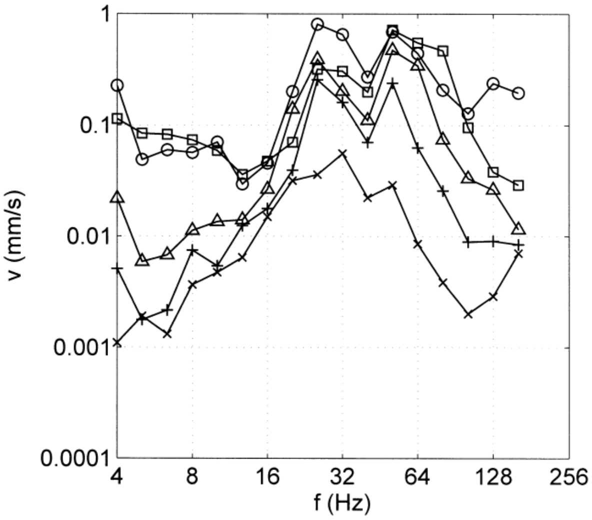

(c)

Figure 1. Train induced ground vibration, from a passenger train with 125 km/h a) Site W [7], b) site L, and c) from a high-speed train with 300 km/h in Spain [8], one-third of octave band spectra at 3 to 50 m distances from the track.

2 Methods

The railway track is analysed by a multi-beam on soil model [19] which yields the following equation in frequency-wavenumber domain (ω,ξ)

$$(\mathbf{EI}\xi^4 + \mathbf{K_{TS}}(\omega,\xi))\mathbf{u}(\omega,\xi) = \mathbf{F'_T}(\omega,\xi). \quad (1)$$

for the displacements **u** and the forces **F'$_\mathbf{T}$**. The dynamic stiffness of the wheel-rail contact point K_T is calculated by the wavenumber integral

$$\frac{1}{K_T(\omega)} = \frac{u_\mathrm{R}}{F_T}(\omega) = \frac{1}{2\pi}\int_{-\infty}^{\infty} \mathbf{e_1}^\mathrm{T}(\mathbf{EI}\xi^4 + \mathbf{K_{TS}}(\omega,\xi))^{-1}\mathbf{e_1}\mathrm{d}\xi. \quad (2)$$

with the matrices of the bending stiffness **EI** and the track-soil stiffness $\mathbf{K}_{\mathbf{TS}}$. The force transfer H_T of the track between the track force F_T and soil force F_S is calculated by

$$F_{\mathrm{S}}(\omega) = k_{\mathrm{S}}(\omega, \xi = 0)\mathbf{e_n}^{\mathrm{T}}\mathbf{K}_{\mathrm{TS}}(\omega, \xi = 0)^{-1}\mathbf{e_1}F_{\mathrm{T}} = H_{\mathrm{T}}(\omega)F_{\mathrm{T}}(\omega) \qquad (3)$$

(k_S is the soil stiffness $\mathbf{e_1}$,$\mathbf{e_n}$ are the base vectors for the top and the bottom of the track.) The track force follows from the irregulrities s and the vehicle-track interaction H_V as

$$F_{\mathrm{T}}(\omega) = -\frac{K_{\mathrm{V}}(\omega)K_{\mathrm{T}}(\omega)}{K_{\mathrm{V}}(\omega)+K_{\mathrm{T}}(\omega)}s(\omega) = H_{\mathrm{V}}(\omega)\, s(\omega) \qquad (4)$$

where K_V is the dynamic stiffness of the vehicle (the wheelset).

The track filtering [12] for geometric track support errors s_S to rail errors s_R

$$s_R(\omega) = \mathbf{e_1}^T\left(\mathbf{EI}\xi^4 + \mathbf{K_{TS0}}(\xi)\right)^{-1}\mathbf{e_n}k_{S0}(\xi)s_S = H_{sT}(\omega = \xi v_T)s_S. \qquad (5)$$

The track filtering for a relative stiffness variation k_1/k_0 can be derived by a two-step linear perturbation analysis as

$$s_R(\omega) = -\frac{F_0 k_0}{2\pi}\int_{-\infty}^{\infty}\mathbf{e_1}^{\mathbf{T}}(\mathbf{EI}\xi^4 + \mathbf{K}_0)^{-1}\mathbf{e_n}\mathbf{e_n}^{\mathbf{T}}(\mathbf{EI}(\xi - \xi_V)^4 + \mathbf{K}_0)^{-1}\mathbf{e_1}\, d\xi\, k_1/k_0 \qquad (6)$$

with the static axle load F_0, and the static stiffness k_0 and $\mathbf{K_0}$.

For the effect of the varying support stiffness on the wave propagation [13], the passage of the static train loads is represented by a number of pulses at a line of discrete excitation points. The passage of a train yields impulses F_0dt on the track due to the static axle load F_0. The length dt of the impulse follows from the distance dy of the discrete excitation points and the train speed v_T as dt = dy/v_T. The impulse on the rail is a Dirac function $\delta(t)$. The bending stiffness of the track filters out the high frequency content of this infinitely sharp impulse. This is included by the filter function H_T (= H_{sT}). The impulses at different places y_j are applied at different times $t_j = y_j/v_T$. The delay time t_j has been included in frequency domain as the factor $\exp(-\mathrm{i}2\pi f t_j)$. Then the response at a point x to the sequence of impulses due to a single axle is given as the spectral density

$$u(x,f) = H_T(f)\, F_0 \mathrm{d}t \sum_{j=-n/2}^{+n/2} H_S(x, y_j, f)\exp(-\mathrm{i}2\pi f t_j) \qquad (7)$$

$H_S(x, y_j, f)$ is the transfer function of the regular [22] or irregular [20] soil (see the finite element model in Fig. 2) which is summed up for the n+1 excitation points y_j. The particle velocity response $v(x,f)$ of a whole train follows by the multiplication with $\mathrm{i}2\pi f$ and the axle-sequence spectrum $X(f)$ [10,15].

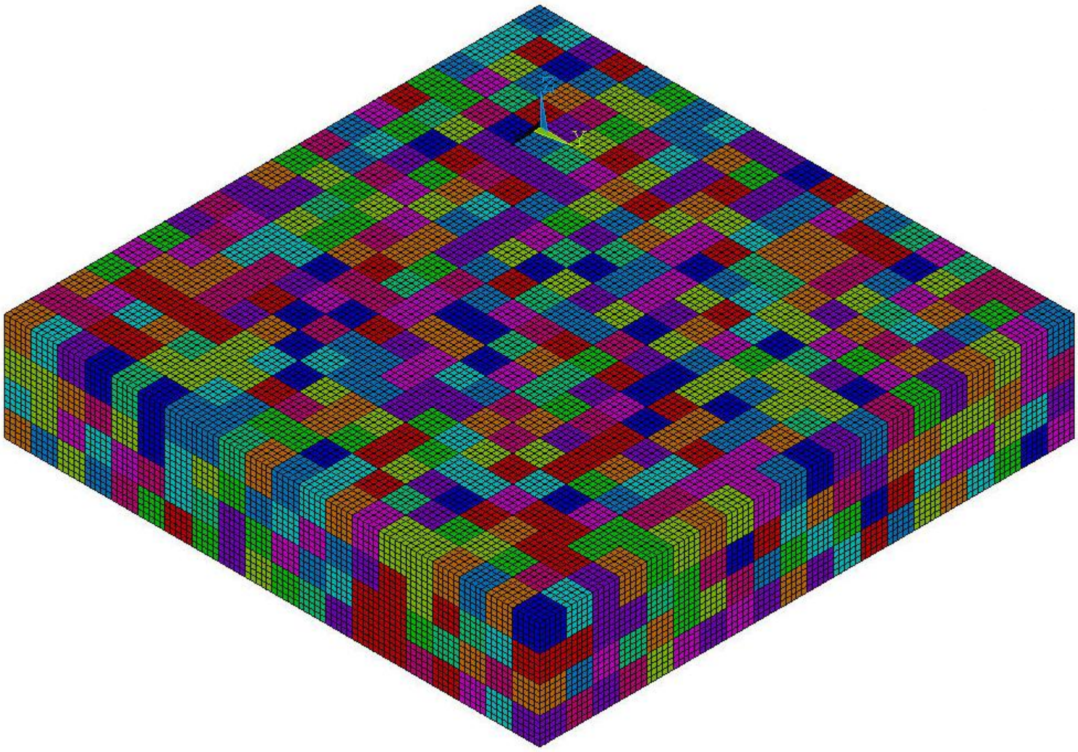

Figure 2. The 100 m x 100m x 20 m wide finite-element model of the soil, different materials are arbitrarily and equally distributed on the cubical subregions.

3 Results

The dynamic loads from vehicle and track irregularitries are demonstrated by results of axle box measurements (Fig. 3).The loads are at about $F \leq 1$ kN per one-third octave band at frequency below 50 Hz and increase to $F \leq 3$ kN above 50 Hz.The maxima of the sleeper passage can be found at 32 to 80 Hz for train speeds of 63 to 160 km/h.The dynamic load amplitudes strongly increase with the train speed, at low frequencies stronger than at high frequencies.

Figure 4 shows the result of the superposition of axle pulses. At low frequencies below 10 Hz, the quasi-static response shows a regular pattern of amplitudes strongly decreasing with frequency and distance.The amplitudes above 10 Hz (between 10 and 32 Hz) are not a regular response to the axle pulses, but an irregular response due to the random stiffness variation. As the track support or the soil has some random variations of the stiffness, the pulse responses along the track vary to some extent. Therefore, parts of the pulse responses are not superposed regularly, but remain with the higher frequencies of the axle pulses. The mid-frequency component (the assumed scattered axle impulses) consists of 3 or 4 elevated thirds of octaves. The maximum amplitudes are enclosed by two clear minima which are even more characteristic and determined by the distance l_A between two axle in a bogie. The frequencies of the minima depend on the train speed as f_{min1}/Hz = $v_T/2l_A$. ≈ v_T/20 km/h, and the second minimum is at the threefold frequency $f_{min2} \approx 3\ f_{min1}$. The characteristic frequency range is shifted with the train speed.

It has been found from calculation and measurements that this stochastic mid-frequency component is reduced by a stiffer soil [19], by a stiffer track support, by the distance from the track (less strong than for dynamic loads [5]), by a plate under the ballast [6] or by a slab track [23]. The combination of a layered soil and an increase of train speed leeds to extremely different amplitude speed relations [7].

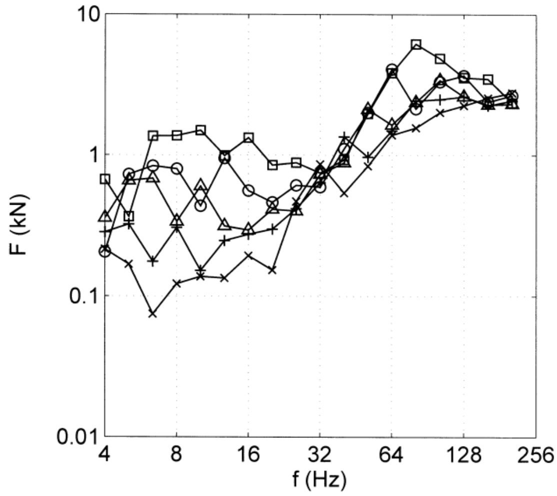

Figure 3. Dynamic axle loads for × 63, + 80, △ 100, ○ 125, □ 160 km/h train speed, evaluated from axle-box measurements.

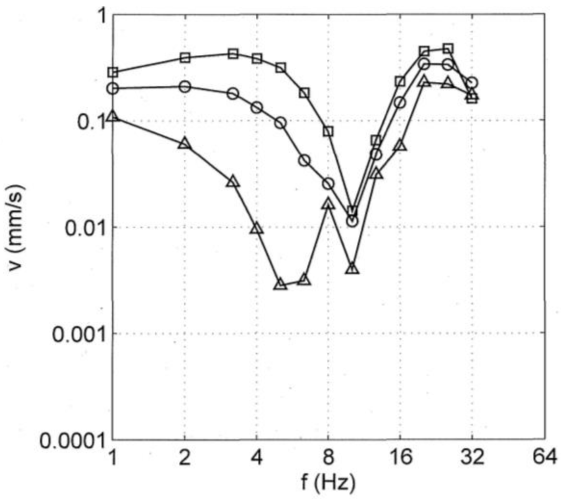

Figure 4. Calculated ground vibrations from a varying track support and soil stiffness, at 3, 5 and 10 m from the track, 200 km/h train speed.

4 Conclusions and Contributions

The scattered axle pulses by a varying track and soil stiffness constitute an important part of the train induced ground vibration. This assumption has been checked by several theoretical and experimental research items.

1. The vehicle dynamics (rigid or flexible car-body, rigid bogie, and flexible wheelset eigenfrequencies have no or only a minor influence on the dynamic load amplitudes [13].
2. The dynamic axle loads are evaluated from axle-box measurements for several sites in Germany and Switzerland. At the same sites, dynamic axle loads are back-calculated from the measured ground vibrations and the transfer functions of the respective soils. The axle loads from the ground vibrations are higher than from the axle-box measurements [5,24] so that other excitations than dynamic axle loads must exist.
3. Moreover, a general trend of the dynamic loads (≤ 1 kN) has been observed, which has been exceeded by back-calculated axle loads at some more ground-vibration measurement sites (Fig. 5) [13].
4. For one of these sites (site W), a detailed forward analysis has been performed for dynamic axle loads from irregularities and for the scattered axle pulses. The (measured) irregularities cannot generate the higher measured ground vibration amplitudes whereas the scatterd axle pulses can (Fig. 6) [19].
5. The early ICE measurements have been re-analysed in [7]. The almost constant amplitudes with increasing train speed fit well to the scattered axle impulses which have almost constant force amplitudes. Dynamic loads from track irregularities should increase with the square of the train speed and therefore could not be the source of this mid-frequency vibration (Fig. 7b,c).
6. Moreover, the different amplitude-speed behaviour can well be explained with the mid-frequency ground vibration component and its position below (Fig. 7a) or above (Fig. 7b,c) the layer frequency of the soil. The strong increase of the transfer function of the soil below the layer frequency yields a strong increase of the mid-frequency ground amplitudes at lower speeds with a maximum around the layer frequency. The constant transfer functions of the soil at higher frequencies yield constant ground amplitudes at higher train speeds (Fig. 7c) [7].
7. The mitigation effect of ballast plates and slab tracks has been analysed theoretically and experimentally showing the reduction in the specific mid-frequency region (Fig. 8).

All these observations lead to the conclusion that the scattered axle impulses are present and often dominant in the train-induced ground vibration.

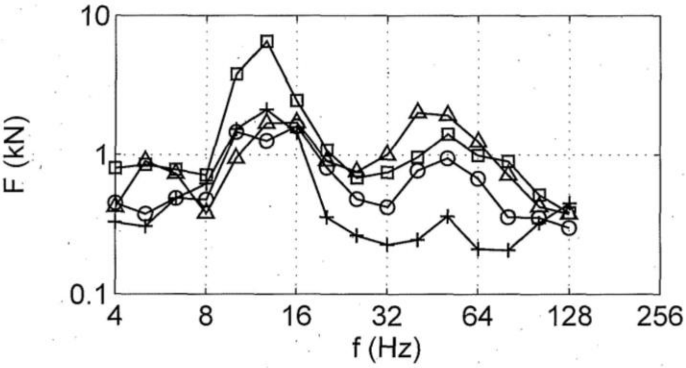

Figure 5. Back-calculated axle loads at site □ W, ○ H, △ N, + L, raised amplitudes between 10 and 16 Hz, train speed 120-160 km/h.

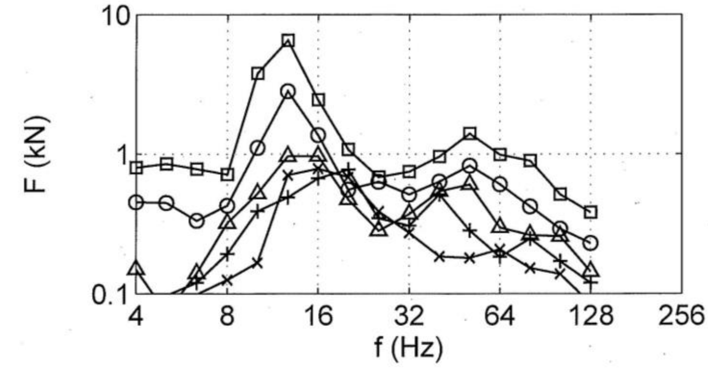

Figure 6. Back-calculated axle loads at site W for × 63, + 80, △ 100, ○ 125, □ 160 km/h train speed.

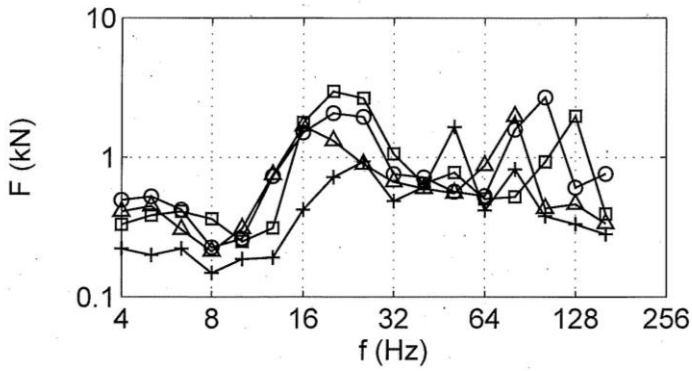

(a)

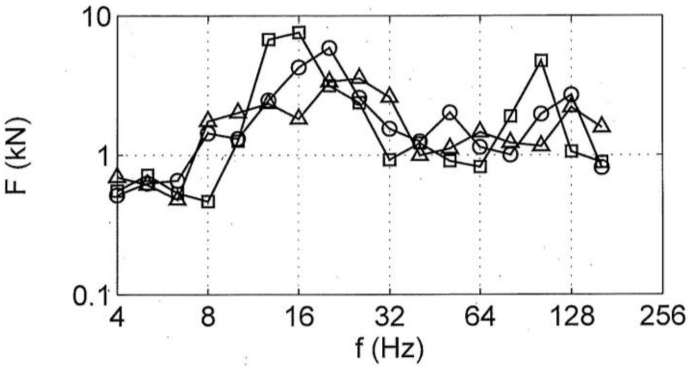

(b)

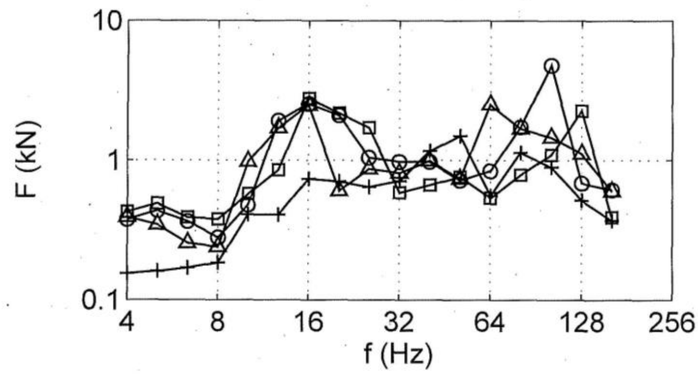

(c)

Figure 7. Back-calculated axle loads a) at site W* (layer of 5 m) for ＋ 100, △ 160, ○ 200, □ 250 km/h train speed, raised amplitudes constantly between 16 and 25 Hz, b) at site W (layer of 10 m) for △ 200, ○ 250, □ 300 km/h train speed, raised amplitudes shifted from 12-16 to 16-20 and 20-32 Hz, c) at site W for ＋ 100, △ 150, ○ 200, □ 250 km/h train speed, raised amplitudes shifted from 8-12, to 10-16, 12-20 and 16-25 Hz.

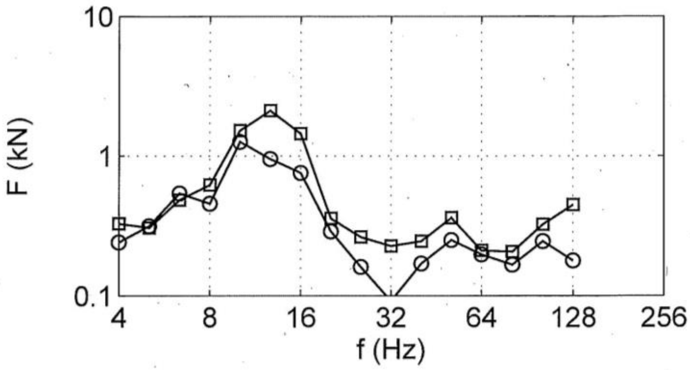

Figure 8. Back-calculated axle loads at site L, □ without, ○ with under-ballast plate, raised or reduced amplitudes between 10 and 16 Hz, train speed 120 km/h.

References

[1] G. Huber, "Erschütterungsausbreitung beim Rad/Schiene-System", PhD Thesis, University Karlsruhe, 1988.

[2] L. Auersch, "Zur Entstehung und Ausbreitung von Schienenverkehrs-erschütterungen: Theoretische Untersuchungen und Messungen am Hoch-geschwindigkeitszug Intercity Experimental", BAM-Forschungsbericht 155, 1988.

[3] M. Heckl, G. Hauck, R. Wettschureck, "Structure-borne sound and vibration from rail traffic", Journal of Sound and Vibration, 193, 175-184, 1996.

[4] L. Auersch, "Parametric excitation of rail-wheel-system: Calculation of vehicle–track–subsoil-dynamics and experimental results of the high-speed train Intercity experimental", Archive of Applied Mechanics, 60, 141–156, 1990 (in German).

[5] L. Auersch, "Realistic axle-load spectra from ground vibrations measured near railway lines", International Journal of Rail Transportation, 3 , 180-200, 2015.

[6] L. Auersch, "Fast trains and isolating tracks on inhomogeneous soils", In V. Krylov (Ed.): "Ground Vibrations from High-Speed Railways: Prediction and Mitigation", ICE Publishing, London, 27-76, 2019.

[7] L. Auersch, "Train induced ground vibrations: different amplitude-speed relations for two layered soils", Journal of Rail and Rapid Transit, 226, 469-488, 2012.

[8] A. Romero, "Predicción, medida experimental y evaluación de las vibraciones producidas por el tráfico ferroviario", PhD Thesis, University of Sevilla, 2012.

[9] D. Connolly, P. Alves Costa, G. Kouroussis, P. Galvin, P. Woodward, O. Laghrouche, “Large scale international testing of railway ground vibrations across Europe”, Soil Dynamics and Earthquake Engineering, 71, 1-12, 2015.

[10] L. Auersch, “The excitation of ground vibration by rail traffic: Theory of vehicle-track-soil interaction and measurements on high-speed lines”, Journal of Sound and Vibration 284, 103-132, 2005.

[11] R. Garburg, C. Frank, and M. Mistler: Investigation of vibration mitigation by concrete trough with integrated under ballast mats for surface-railways. Proc. Int. Workshop on Railway Noise and Vibration, KU Leuven, 2019, 1-8.

[12] L. Auersch, “Excitation of ground vibration due to the passage of trains over a track with trackbed irregularities and a varying support stiffness”, Vehicle System Dynamics, 53, 1-29, 2015.

[13] L. Auersch, “The role of vehicle dynamics in train-induced ground vibrations and the detection of irregular axle-pulse responses due to a varying track stiffness”, Rail and Rapid Transit, 236, 2022. (Accepted for publication).

[14] X. Sheng, C. Jones, D. Thompson, “Comparison of a theoretical model for quasi-statically and dynamically induced environmental vibration from trains with measurements”, Journal of Sound and Vibration, 267, 621-635, 2003.

[15] L. Auersch, “Ground vibration due to railway traffic – the calculation of the effects of moving static loads and their experimental verification”, J. of Sound and Vibration, 293, 599–610, 2006.

[16] G. Lombaert, G. Degrande, “Ground-borne vibration due to static and dynamic axle loads of InterCity and high-speed trains”, Journal of Sound and Vibration, 319, 1036-1066, 2009.

[17] L. Auersch, “Theoretical and experimental excitation force spectra for railway induced ground vibration – vehicle-track soil interaction, irregularities and soil measurements”, Vehicle System Dynamics, 48, 235–261, 2010.

[18] H. Hunt, “ Types of rail roughness and the selection of vibration isolation measures”, In Noise and Vibration Mitigation for Rail Transportation Systems; Notes on Numerical Fluid Mechanics and Multidisciplinary Design, Schulte-Werning B. et al. Eds.; Springer: Berlin, Heidelberg, 99, 341-347, 2008.

[19] L. Auersch, “Different types of continuous track irregularities as sources of train-induced ground vibration and the importance of the random variation of the track support”, Applied Sciences 12, 12031463, 2022.

[20] L. Auersch, “Train-induced ground vibration due to the irregularities of the soil”, Soil Dynamics and Earthquake Engineering 140, 106438, 2021.

[21] V. Krylov, “Ground vibration boom from high-speed trains: Prediction and reality,” Acoustics Bulletin, 23, 15-22, 1998.

[22] L. Auersch, “Wave propagation in layered soil: theoretical solution in wavenumber domain and experimental results of hammer and railway traffic excitation”, Journal of Sound and Vibration, 173, 233-264, 1994.

[23] L. Auersch, “Characteristics of train passages over slab tracks from measurements and different track-soil models: Damage detection and ground vibration reduction”, J. Rail and Rapid Transit, 234, 142–160, 2020.

[24] L. Auersch, “Emission of train-induced ground vibration — Prediction of axle-load spectra and its experimental verification”. International Journal of Acoustics and Vibrations 22, 74-83, 2017.